

BACK ANGLE ANOMALOUS SCATTERING IN AN ODD MASS SYSTEM : $^{19}\text{F} + ^{12}\text{C}$

C. F. MAGUIRE and J. H. HAMILTON

Vanderbilt University, Physics Department, Nashville, TN 37235, USA

(Received 17 February 1986)

One of the most striking discoveries in heavy-ion induced reactions was the observation by Braun-Munzinger et al. [1] of anomalously large yields at backward angles in heavy-ion elastic and inelastic scattering. As first seen in the $^{28}\text{Si} + ^{16}\text{O}$ system (see Fig. 1), unexpected structure and enhancement occur in the backward hemisphere differential cross sections. Whereas the forward angle cross sections can be well fitted by a standard strong absorption optical potential [2], fitting the back angle yields requires new physics input such as the addition of a Regge pole [3-4]. Without such a refinement, the predicted back angle cross sections would be several orders of magnitude below that which is observed. An even more telling discovery, by Barrette et al [5] and by Clover et al. [6], was the association of the enhanced back angle yields with structures in the near 180° excitation functions $^{28}\text{Si} + ^{16}\text{O}$ and $^{28}\text{Si} + ^{12}\text{C}$ (Figs. 2 and 3). One observes in these excitation functions correlated, broad (1-2 MeV) gross structures, too wide to be compound elastic in origin and too narrow to come from conventional direct reaction processes. The importance of this discovery is that while simply weakening the absorption of the optical potential (surface transparency) is sufficient to enhance the predicted back angle cross sections, such optical potentials cannot reproduce the observed structures in the excitation function data.

Correlated excitation function structures ("resonances") have also been observed by Ford et al. [7] in $^{20}\text{Ne} + ^{12}\text{C}$ and $^{24}\text{Mg} + ^{12}\text{C}$.

The phenomenon was seen to disappear almost entirely or at least to become substantially diminished when a non- α -conjugate nucleus was introduced: e. g. $^{28}\text{Si} + ^9\text{Be}$ or ^{13}C (Fig. 4, Refs. 8, 9), $^{28}\text{Si} + ^{18}\text{O}$ (Ref. 10), $^{27}\text{Al} + ^{12}\text{C}$ (Ref. 11), $^{29,30}\text{Si} + ^{16}\text{O}$ (Ref. 12), and $^{32}\text{S} + ^{13}\text{C}$ (Ref. 9). Even for such α -conjugate systems such as $^{32}\text{S} + ^{12}\text{C}$

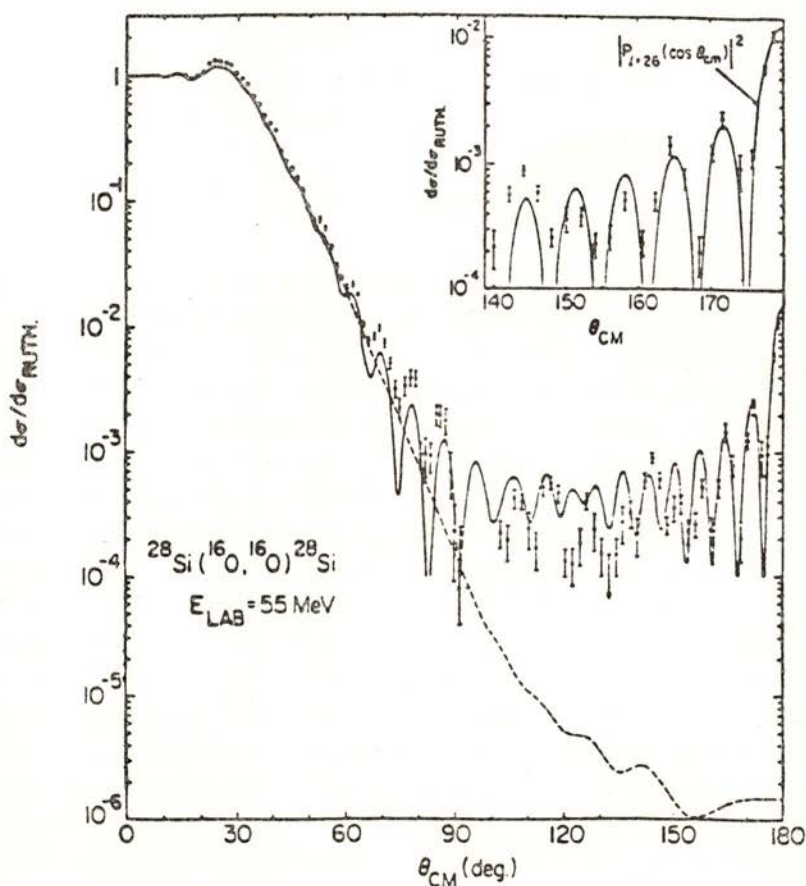


Fig. 1 — Elastic angular distribution for $^{16}\text{O} + ^{28}\text{Si}$ at a lab energy of 55 MeV (Ref. 1). The dashed line represents the predictions of the strongly absorbing optical potential set E18 (Ref. 2) which fits the forward angle region but can not fit the interior and back angle regions. The solid line is the prediction of optical potential set E18 modified to include a Regge pole contribution to the scattering matrix elements. In the inset is shown an expanded view of the back angle data which can be fitted by a $P_{L,0}(\cos \Theta)$ function.

(Refs. 8, 9, 13), $^{40}\text{Ca} + ^{12}\text{C}$ (Refs. 8, 14), and $^{24}\text{Mg} + ^{12}\text{C}$ (Fig. 5), the gross structures in the excitation function data are not nearly as prominent as in $^{28}\text{Si} + ^{16}\text{O}$ or ^{12}C . A major question arising from these experiments is whether the back angle anomalies represent the existence of resonances in the composite systems such as the quasi-molecules postulated for $^{16}\text{O} + ^{16}\text{O}$ scattering, or do they represent unknown characteristics of the ion-ion potential.

In an effort to further the understanding of this phenomenon we at Vanderbilt, in collaboration with members of Los Alamos and Brookhaven National Labs, have begun to study the $^{19}\text{F} + ^{12}\text{C}$ odd mass system. On the basis of the preceding discussion, one

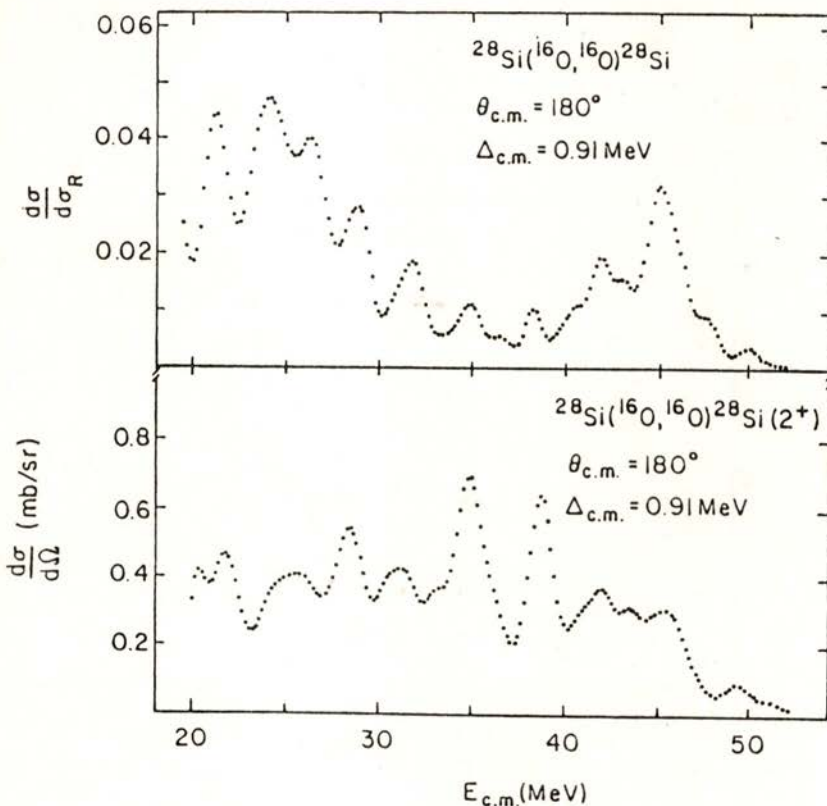


Fig. 2—Elastic and inelastic excitation function data for the system $^{28}\text{Si} + ^{16}\text{O}$. The experimental data have been averaged over 0.91 MeV (c. m.) to emphasize the gross structures present in the data. (From Ref. 15).

might have anticipated that at best only weak anomalous structure would be present. The situation is further complicated because of the existence of two low-lying states in ^{19}F at 110 ($1/2^-$) and 197 ($5/2^+$) keV. In order to resolve this pair of states from the ground state and each other, it is necessary to use very thin

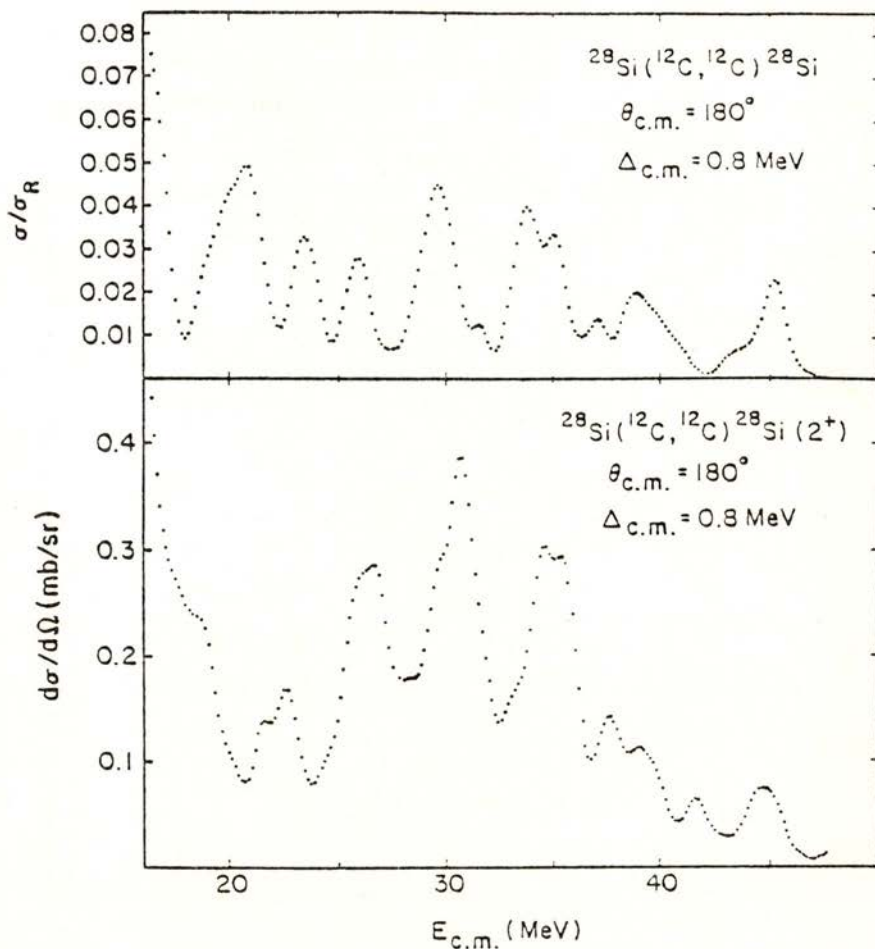


Fig. 3—Elastic and inelastic excitation function data for the system $^{28}\text{Si} + ^{12}\text{C}$, where the actual experimental data are averaged over 0.80 MeV (c. m.) to emphasize the gross structure. Without this averaging procedure, fine structures of the order 100 keV would be visible. (From Ref. 15).

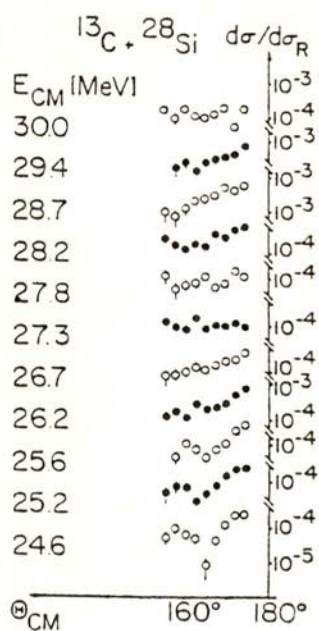


Fig. 4 — Elastic excitation function data for the system $^{28}\text{Si} + ^{13}\text{C}$ taken at near 180° (Ref. 8). Note that compared to the $^{28}\text{Si} + ^{12}\text{C}$ data in the previous figure, these cross sections are two orders of magnitude smaller. No structure is apparent in the excitation function nor is there pronounced oscillation in the angular distributions.

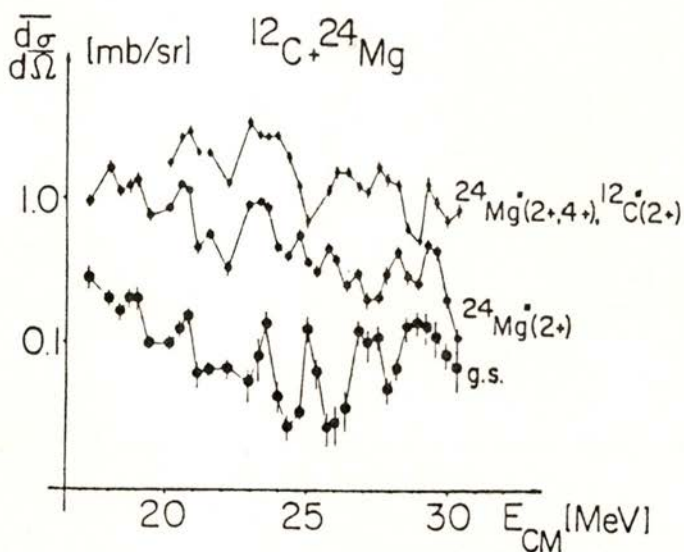


Fig. 5 — Elastic and inelastic excitation function data for the system $^{24}\text{Mg} + ^{12}\text{C}$ taken near 180° (Ref. 7). The pattern here is more irregular than in $^{28}\text{Si} + ^{16}\text{O}$ or ^{12}C .

(10 $\mu\text{g}/\text{cm}^2$) targets. One cannot thus take advantage of the automatic energy averaging property of the thick (200 $\mu\text{g}/\text{cm}^2$) targets normally used in this type of experiment. Furthermore,

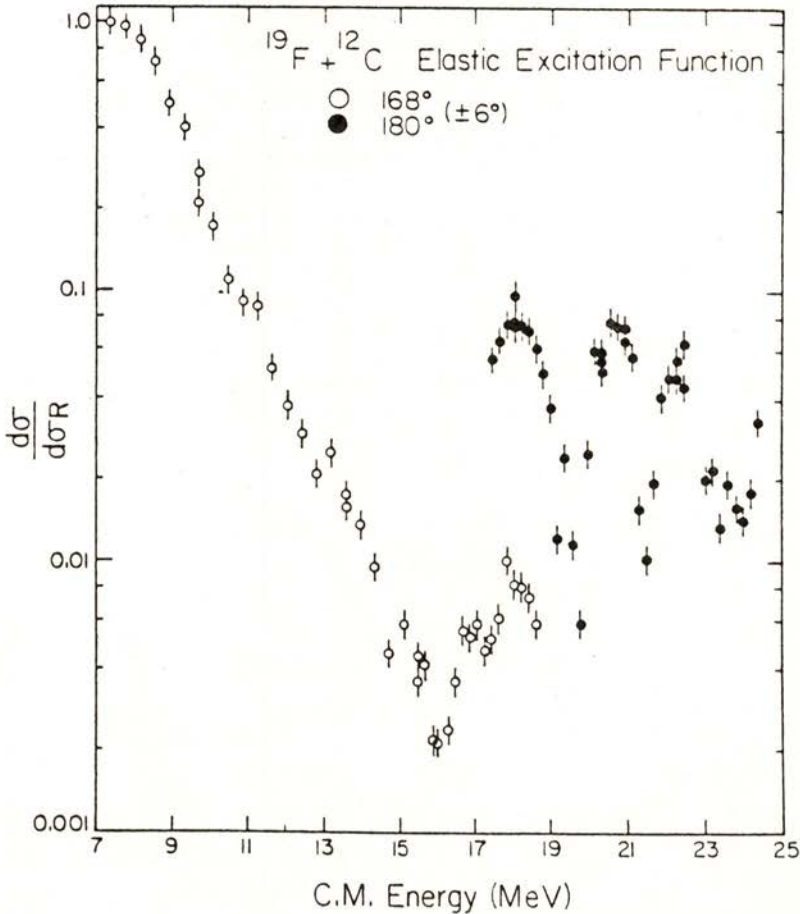


Fig. 6 — Elastic excitation function data for the system $^{19}\text{F} + ^{12}\text{C}$ taken at 180 and at 168° c. m.

small energy steps must be taken in the excitation function in order to account for the possible presence of fine structure in the data. Rather startlingly the data (Fig. 6) turned out to be com-

pletely different from what we expected. For this odd mass system the 180° gross structure excitation functions anomalies (elastic-to-Rutherford and peak-to-valley ratios) exceed even those of the prototype $^{28}\text{Si} + ^{16}\text{O}$ or ^{12}C systems. Three very prominent structures are apparent in the elastic and inelastic excitation function where the elastic yield at 180° peaks between 6 and 8 % of the Rutherford scattering value and the excursion in the cross section from maximum to minimum is more than a factor of 20:1.

These excitation function data were measured at Brookhaven National Laboratory using a ^{19}F beam on a natural carbon target.

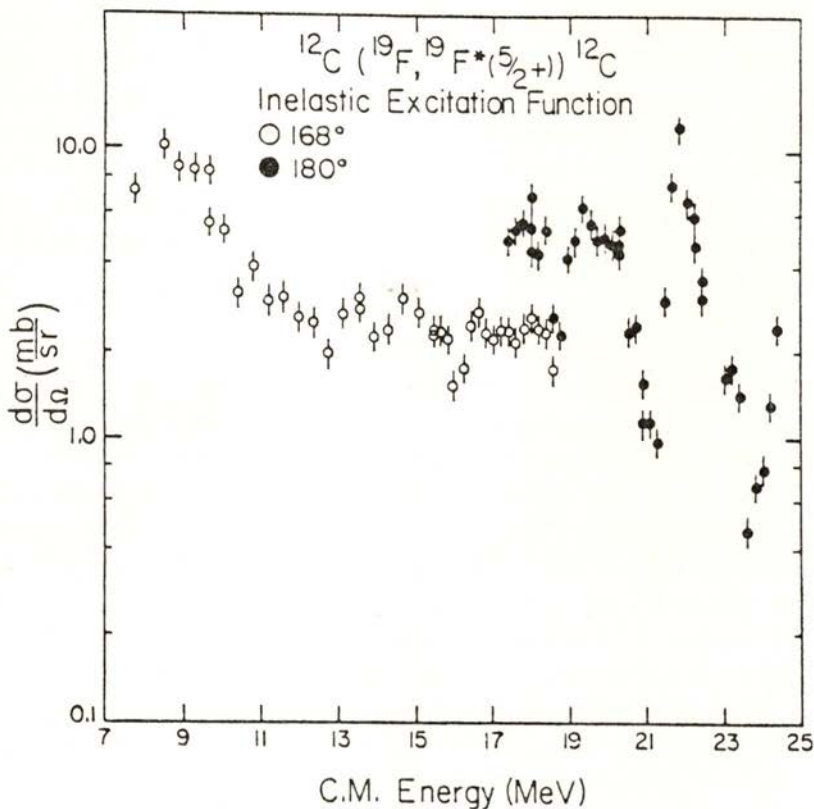


Fig. 7 — Inelastic excitation function data for the system $^{19}\text{F} + ^{12}\text{C}$ populating the second excited state of ^{19}F .

The forward recoiling ^{12}C ions were momentum analyzed in the BNL QDDD magnetic spectrometer positioned at 0° ($\pm 3^\circ$). A dual chamber gas detector system was used to identify the reaction products and it was found necessary to introduce nickel absorber foils (64 to $135\ \mu$ thickness) to prevent slit scattered primary beam from saturating the detector. Because of this degraded primary beam, no data could be taken below 45 MeV incident energy at 0° . Excitation data were taken between 19 and 46.5 MeV incident energy at 6° lab (168° c. m.), where there was no slit scattering problem.

As can be seen in Fig. 6, for the system $^{19}\text{F} + ^{12}\text{C}$ the gross structure in the elastic scattering is by far the dominant feature, almost completely overwhelming any trace of intermediate structure. Three very prominent structures are seen at center-of-mass energies of 18.0, 20.7, and 22.1 MeV, and there is the hint at the highest measured energy that a fourth structure will occur. In the 168° excitation function data, the 18.0 MeV structure is a factor of 10 below the 180° yield, indicating that the angular distribution at this energy must be backward rising. The 168° data also give some evidence of structures at lower energies, perhaps at 11.3, 13.0, and very slightly at 14.9 MeV.

No evidence was found for the excitation of the 110 keV state, as might be expected since this $1/2^-$ level must have a dominant p-shell hole admixture. However, the 197 keV $5/2^+$ state is strongly excited (Fig. 7) and its excitation function data display the same prominent gross structures as in the elastic channel.

Two points are especially striking with regard to these excitation function data. The first is the sheer prominence of the gross structures. The second is their existence in an *odd* mass system, given that a nearby α -conjugate system $^{24}\text{Mg} + ^{12}\text{C}$ displays the phenomenon only relatively weakly. It has been thought that a necessary condition for the enhanced cross sections at back angles is a weak absorptive term in the optical potential. The absorption in odd mass systems should be greater than in the more strongly bound α -conjugate systems. In the face of such increased absorption, the diminution of the back angle anomalies in non- α -conjugate systems could be understood. The present data would appear to seriously undermine that argument.

A characteristic feature of the back angle anomaly is the highly oscillatory pattern of the near 180° differential cross section. In fact the shapes there can be fitted well by the square of a single Legendre polynomial $P_{L,0}^2(\cos \theta)$, (see inset, Fig. 1). At first sight this might lend credence to the idea of isolated resonances as the interpretation for the phenomenon. For spin-zero on spin-zero scattering, the differential cross section is given by:

$$\frac{d\sigma}{d\Omega}(\theta)_{\text{el}} = |f_{\text{C}}(\theta) + (2ik)^{-1} \sum_L (2L+1) \exp(2i\sigma_L) (S_L - 1) P_{L,0}(\cos \theta)|^2 \quad (1)$$

where $f_{\text{C}}(\theta)$ and σ_L are the Coulomb scattering amplitude and phase, respectively, and S_L is the scattering matrix element for partial wave L . Since at 180° the Legendre polynomials vary as $(-1)^L$, there will tend to be a high degree of cancellation when the S_L vary smoothly in magnitude and phase, as usually is the case in heavy-ion elastic scattering. On the other hand, should one of the S_L become predominant, then the cross section at back angles will be very much a $P_{L,0}^2(\cos \theta)$ function. In the case of $^{28}\text{Si} + ^{16}\text{O}$ an L sequence of 9, 16, 16, 22, and 24 was extracted [15] from angular distributions taken at the maxima of the gross structures shown in Fig. 2. Although it turns out that these L values follow closely the grazing partial wave values, their irregular sequence is difficult to understand in terms of a band of resonant states. More seriously, Braun-Munzinger et al. [15] have shown that midway between two of these structures, the measured angular distribution cannot be described in terms of the interference of the two adjacent "resonant" structures. For $^{28}\text{Si} + ^{12}\text{C}$ and for $^{32}\text{S} + ^{12}\text{C}$, the L sequence was also determined to be irregular, and from 1 to 5 units *below* the grazing partial wave value. Most erratic of all is the behavior of the $^{20}\text{Ne} + ^{12}\text{C}$ system for which the L sequence is 15, 14, and 19 in an energy region where the $l_{\text{gr}} = 20-21$. It should be noted that $^{20}\text{Ne} + ^{12}\text{C}$ is the α -conjugate neighbor of the $^{19}\text{F} + ^{12}\text{C}$ system presently under study.

Subsequent to the excitation function data analysis, we conducted an angular distribution experiment for $^{19}\text{F} + ^{12}\text{C}$ at Los

Alamos National Laboratory. Angular distribution data were measured between 130 and 170° c.m. at the maxima of the three gross structures seen in the elastic excitation function data at 180° . A fourth angular distribution was measured at an intermediate energy, "off-resonance", of 21.3 MeV. These data for the ground and second excited state of ^{19}F are illustrated in Figs. 8 and 9.

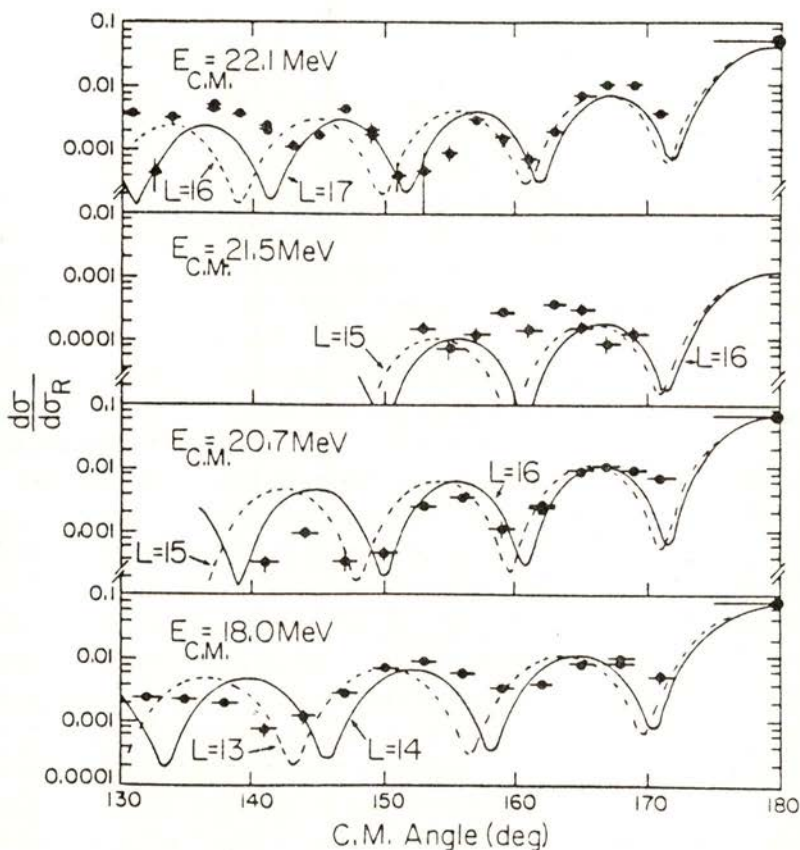


Fig. 8 — Elastic angular distribution data for the system $^{19}\text{F} + ^{12}\text{C}$ measured at the maxima of the gross structures seen in the 180° excitation function. The lines drawn through the data point represent $P_{L,0}^2(\cos \Theta)$ fits to the oscillatory pattern. The 21.5 MeV data set correspond to a minimum in the excitation function data and no backward rising of the cross section is apparent.

At the three "resonance" energies both groups are seen to display oscillatory, backward rising angular distributions whose frequency increases with increasing beam energy. At the intermediate energy point, no oscillation is apparent.

Because of the spin 1/2 nature of ^{19}F , the formula for the

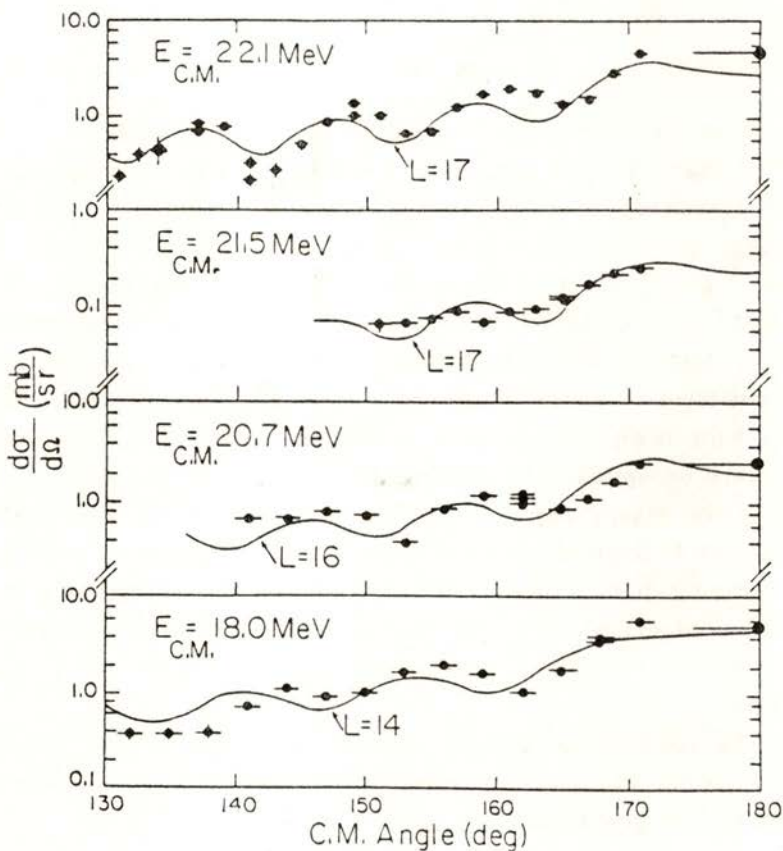


Fig. 9— Inelastic angular distribution data for the system $^{19}\text{F} + ^{12}\text{C}$ exciting the second excited state of ^{19}F at 0.197 MeV ($5/2^+$). The lines through the data represent an incoherent sum of associated Legendre polynomials having the same L values as in the elastic angular distribution fits. The exception is the "off-resonance" energy set (21.5 MeV) for which an L value of 17 is represented.

elastic differential cross sections is slightly more complicated than for spin-zero on spin-zero scattering:

$$\frac{d\sigma}{d\Omega}(\theta)_{\text{el}} = \sum_{m_a, m'_a} |f_C(\theta) \delta_{m_a, m'_a} + (2ik)^{-1} \sum_{J, L} \langle L \ 1/2 \ 0 m_a | J m_a \rangle \langle L \ 1/2 (m_a - m'_a) m'_a | J m_a \rangle \sqrt{(L - M')! / (L + M')!} (2L + 1) e^{2i\sigma_L} (S_L^J - 1) P_{L, M'}(\cos \theta)|^2 \quad (2)$$

$$M' = |m_a - m'_a| = 0 \text{ or } 1$$

Now there is a sum over the total channel spin J and the partial wave L , and associated Legendre polynomials appear as well. However, for a given channel spin and parity, J_π , there is a unique partial wave L which contributes. (This is not true for spins higher than $1/2$). In terms of the resonance model, then, it is still correct to interpret the back angle angular distributions with a single L value. More restrictively, if the S matrix elements are assumed to be generated by a *central* ion-ion potential, then the J sum in Eq. (2) collapses to just an L sum, as in Eq. (1) for spin-zero on spin-zero scattering. In this manner we obtained the fits to the elastic angular distributions as shown in Fig. 8. The extracted L sequence here is quite regular and tracks well with the grazing partial wave value. Again, given the highly erratic behavior of neighboring system $^{20}\text{Ne} + ^{12}\text{C}$, this regular sequence in the $^{19}\text{F} + ^{12}\text{C}$ differential cross sections comes as a great surprise.

The oscillatory inelastic angular distributions can also be fitted within the single L model. The formula for the inelastic excitation is given by:

$$\frac{d\sigma}{d\Omega}(\theta)_{\text{inel}} = \sum_{m_a, m'_a} |(2ik)^{-1} \sum_{J, L, L'} \langle L \ 1/2 \ 0 m_a | J m_a \rangle \langle L' \ 5/2 (m_a - m'_a) m'_a | J m_a \rangle \sqrt{(2L + 1)(2L' + 1)} e^{i(\sigma_L + \sigma_{L'})} \sqrt{(L - M')! / (L + M')!} S_{L, L'}^J P_{L', M'}(\cos \theta)|^2 \quad (3)$$

$$M' = |m_a - m'_a| = 0, 1, 2, 3$$

As in the elastic case, only one entrance channel partial wave L contributes for a given channel spin and parity J_π . However, three outgoing partial waves $L' = L - 2, L, L + 2$, can be coupled coherently to produce the differential cross section. If a single L is considered to be dominant in Eq. (3) at back angles, then the allowed Legendre polynomials are in phase and this can lead to a backward rising shape. Indeed, taking only the diagonal $L' = L$ term in Eq. (3) and making an *ad hoc* superposition of $P_{L,M}^2(\cos \theta)$ functions ($M = 0, 1, 2$), we obtain the fits to the inelastic angular distributions shown in Fig. 9. In these fits the $M = 2$ contribution is the most important, the $M = 1$ fills in the oscillations, and the $M = 0$ contribution yields the finite cross section at 180° . (The possible $M = 3$ contribution is ignored as it would not occur in spin-zero on spin-zero scattering). Hence, the fits depicted in Figs. 8 and 9 show that both the elastic and inelastic data are compatible with the interpretation of the same dominant L value. Of course this evidence is not conclusive and there is no prescription yet available for generating the observed sequence of L values.

The discussion so far has concentrated on the single L interpretation of the back angle phenomenon. An alternate explanation, proposed by Dehnhard et al. [16], is that there is a parity dependent component in the ion-ion potential. That is, to a standard optical potential $U(r)$ is added an L dependent term of the form $(-1)^L P U(r)$. The parity coefficient P is of the order 0.01. This approach is amazingly successful in describing the $^{28}\text{Si} + ^{16}\text{O}$ elastic excitation function data, as shown in Fig. 10. The back angle elastic and inelastic angular distributions are also fitted reasonably well [15, 16]. The theoretical justification for this parity dependence is the possible core exchange of a ^{12}C nucleus between the projectile ^{28}Si and the target ^{16}O . Such an exchange would lead to a Majorana component in the interaction potential. The inclusion of parity dependence in the optical potential upsets the delicate cancellation of the $P_{L,0} \cos(\theta)$ in the summation of Eq. (1), leading instead to a coherent enhancement of all L contributions at the back angles. Although this approach is very successful, there is a serious question about the probability of the elastic transfer of a ^{12}C nucleus. The spectroscopic factor must be vanishingly small and it seems unlikely an effective parity

dependence would be present. Nonetheless, this idea has been also used in explaining the $^{32}\text{S} + ^{12}\text{C}$ back angle excitation function with a fair degree of success. As in the case of $^{28}\text{Si} + ^{16}\text{O}$, a positive parity coefficient P was found, meaning that the potential is more attractive for even than for the odd partial waves. Kubono [17] has also studied the question of parity dependence by comparing the 90° and the 180° $^{28}\text{Si} + ^{16}\text{O}$ excitation functions. Contradicting the other two studies, Kubono concluded that the parity coefficient should be negative, more attractive for odd rather than even partial waves.

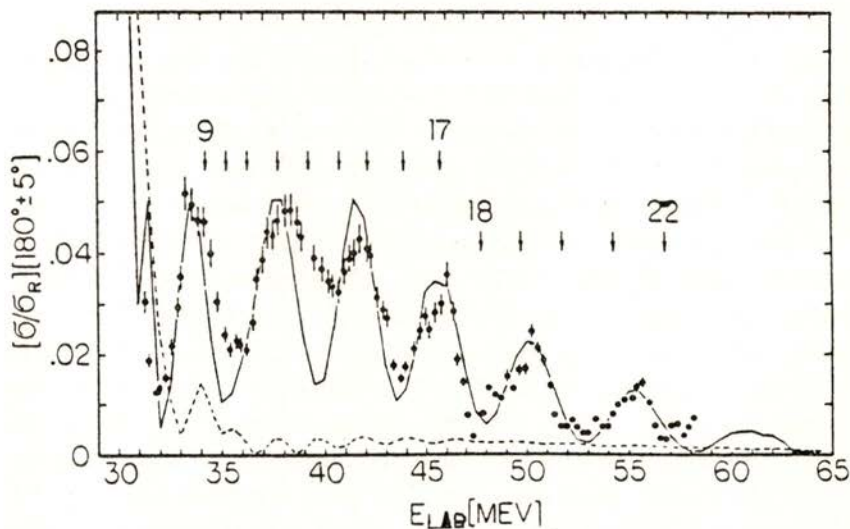


Fig. 10 — The $^{28}\text{Si} + ^{16}\text{O}$ elastic excitation function data at 180° . The solid curve through the data points represents the predictions of the parity dependent optical potential parameter set developed by Dehnhard et al. (Ref. 16). The broken curve represents the predictions of the same optical parameter set with the parity coefficient set to zero. The arrows in the figure represent the positions of the $n=0$ shape resonances of the optical potential for which some of the L values are explicitly written.

We have investigated the question of parity dependence in the $^{19}\text{F} + ^{12}\text{C}$ system with mixed success. The result depends critically on the base optical potential $U(r)$ which is used. Our

first attempt used the parameters of Voos et al. [18] ($V = 100$ MeV, $r_R = 1.19$ fm, $a_R = 0.48$ fm, $W = 23$ MeV, $r_I = 1.26$ fm, and $a_I = 0.26$ fm) which fits the forward angle elastic scattering of $^{19}\text{F} + ^{12}\text{C}$ in the incident energy regime under study here. This potential is rather strongly absorbing and a large parity coefficient ($P = 0.4$) was found to be necessary to enhance the back angle yield to the level observed at 180° (8 % of Rutherford). It then turns out that no structure is produced in the excitation function with this choice of parity dependence. As a function of energy, the predicted back angle yield simply rises monotonically. Our next choice of optical potential was the parameter set used by Dehnhard to fit the $^{28}\text{Si} + ^{16}\text{O}$, for which the real and imaginary depths are a factor of 6 below those of the Voos set. With this new parameter set for $U(r)$, the parity dependence was much more successful in reproducing the $^{19}\text{F} + ^{12}\text{C}$ elastic excitation function data, as can be seen in Fig. 11. We find here also that a positive parity coefficient is necessary, although the coefficient is in this case a factor of 5 reduced from the $^{28}\text{Si} + ^{16}\text{O}$ analysis. If the opposite sign of the parity coefficient is used, the predicted structures become out-of-phase with those shown in Fig. 11. In the present case the parity dependence might arise because of the exchange of a ^7Li core between the ^{19}F and the ^{12}C . While the spectroscopic factor for this exchange might be higher than for ^{12}C in the $^{28}\text{Si} + ^{16}\text{O}$ experiment, the expected low probability for the process remains a troubling question.

Fortunately, an effective parity dependence in the S matrix elements can be obtained without introducing explicitly a parity dependent component in the optical potential. This approach was first developed by Lee [19] and extended by Braun-Munzinger et al. [15] for the $^{28}\text{Si} + ^{16}\text{O}$ data. The basic idea is that there can exist a pocket, of depth and width depending upon the partial wave number L , in the real potential. Incoming partial waves will be reflected at the exterior and interior boundaries of the pocket. Provided that the absorption inside the pocket is not too great, the wave reflected from the interior boundary of the pocket can interfere significantly with the wave reflected from the exterior boundary. With the use of the semi-classical approximation, the S matrix elements are parameterized in this model and a rather good

fit to the excitation function data in $^{28}\text{Si} + ^{16}\text{O}$ can be generated. A qualitative prediction of the model is that since the pocket in the optical potential tends to disappear at higher energies, the

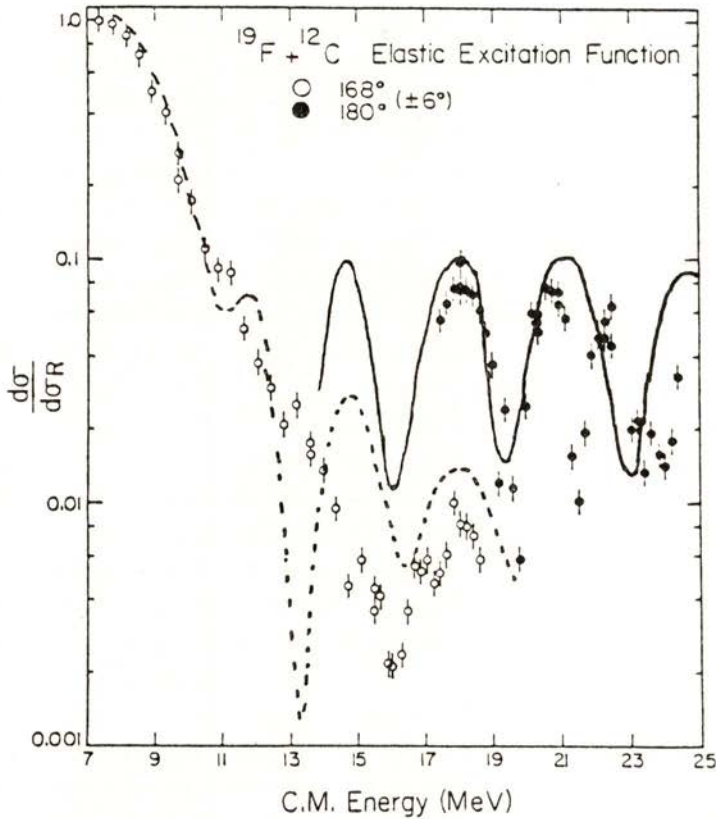


Fig. 11 — Elastic excitation function data for $^{19}\text{F} + ^{12}\text{C}$ fitted with the parity dependent optical potential parameter set developed by Dehnhard et al. [16]. While the qualitative agreement with the data is good, it should be noted that the minimum in the 168° data set near 16 MeV c. m. is predicted too early by this potential set.

back angle phenomenon should diminish also with increasing incident energy. A drawback of the model, however, is that there is no explicit parameterization of the underlying optical potential.

The back angle anomaly is most obvious in the elastic and inelastic channels. Attempts to correlate these structures with other reaction channels have not been particularly fruitful. The best investigated case has been the α -particle transfer reaction channel, $^{24}\text{Mg} (^{16}\text{O}, ^{12}\text{C}) ^{28}\text{Si}$, measured at both forward [20] and backward angles [21]. This reaction channel does show excitation function structures, but there is no clear correlation between those structures and the ones seen in the entrance or exit channel elastic scattering. Recently, Lichtenthaler et al. [22] have performed a two-step α -transfer reaction ($^{12}\text{C} + ^{24}\text{Mg} \rightarrow ^{16}\text{O} + ^{20}\text{Ne} \rightarrow ^{12}\text{C} + ^{24}\text{Mg}$) which would coherently interfere with the elastic channel. This calculation indicated that this interference could account for the intermediate angle oscillations seen in the elastic differential cross section. It was speculated by these authors that the successive transfer of three α -particles could explain the back angle rise in the elastic cross section. Although the idea of α -transfer is of course attractive for the α -conjugate systems, it would not seem to be applicable to the $^{19}\text{F} + ^{12}\text{C}$ elastic scattering. In fact this transfer reaction has been measured at 40, 60, and 68 MeV (Ref. 23) and the cross sections have been found to be rather small compared to the α -transfer cross sections between α -conjugate nuclei. On the other hand, the triton transfer reaction $^{12}\text{C} (^{19}\text{F}, ^{16}\text{O}) ^{15}\text{N}$ is a very strong channel (tens of millibarns) (Ref. 23). This channel could conceivably be interfering with the elastic channel to produce the structures observed in the $^{19}\text{F} + ^{12}\text{C}$ excitation function.

Another avenue of exploration for the understanding of these structures is the light particle emission yields. So far this has not been done for the systems considered so far, but it has been measured in the case of $^9\text{Be} + ^{12}\text{C}$. The back angle elastic yield in this system also exhibits structures [24] which may be related to the elastic transfer of a ^3He . In addition, the α -emission channel has also been observed. There are clear structures in this emission channel, structures which seem to be correlated with those seen in the elastic channel.

The back angle enhancement anomaly in heavy-ion elastic scattering presents a fascinating puzzle for the understanding of heavy-ion interactions. The phenomenon, already known to be

widespread for α -conjugate nuclei is now revealed to occur most prominently in an odd mass system. The present data thus provide a new challenge and new constraints on models proposed to interpret the data.

The work at Vanderbilt University is supported by the U. S. Department of Energy under Contract No. DE-AS05-76ER05034.

REFERENCES

- [1] P. BRAUN-MUNZINGER, G. M. BERKOWITZ, T. M. CORMIER, C. M. JACHINSKI, J. W. HARRIS, J. BARRETTE, and M. J. LEVINE, *Phys. Rev. Lett.*, **38**, 944 (1977).
- [2] J. G. CRAMER, R. M. DEVRIES, D. A. GOLDBERG, M. S. ZISMAN and C. F. MAGUIRE, *Phys. Rev.*, **C14**, 2158 (1976).
- [3] K. McVOY, *Phys. Rev.* **C3**, 1104 (1971).
- [4] K. McVOY, in *Proc. of the Symposium on Heavy-Ion Elastic Scattering*, ed. R. M. DEVRIES (Univ. of Rochester, 1977), p. 430.
- [5] J. BARRETE, M. J. LEVINE, P. BRAUN-MUNZINGER, G. M. BERKOWITZ, J. GAI, J. W. HARRIS and C. M. JACHINSKI, *Phys. Rev. Lett.*, **40**, 445 (1978).
- [6] M. R. CLOVER, R. M. DEVRIES, R. OST, N. J. A. RUST, R. N. CHERRY, JR. and H. E. GOVE, *Phys. Rev. Lett.*, **40**, 1008 (1978).
- [7] J. L. C. FORD, JR., J. GOMEZ DEL CAMPO, D. SHAPIRA, M. R. CLOVER, R. M. DEVRIES, B. R. FULTON, R. OST and C. F. MAGUIRE, *Phys. Lett.* **89**, 48 (1979).
- [8] R. OST, M. R. CLOVER, R. M. DEVRIES, B. R. FULTON, H. E. GOVE and N. J. RUST, *Phys. Rev.* **C19**, 740 (1979).
- [9] Y-d. CHAN, R. J. PUIGH, W. L. LYNCH, M. Y. TSANG and J. G. CRAMER, *Phys. Rev.*, **C25**, 850 (1982).
- [10] P. BRAUN-MUNZINGER and J. BARRETTE in *Proc. of the Symposium on Heavy-Ion Elastic Scattering*, (Univ. of Rochester, 1977), p. 45.
- [11] A. ROY, A. D. FRAWLEY and K. W. KEMPER, *Phys. Rev.*, **C20**, 2143 (1979).
- [12] P. BRAUN-MUNZINGER et al., *Bull. Am. Phys. Soc.*, **24**, 571 (1979).
- [13] C. K. GELBKE, T. C. AWES, U. E. P. BERG, J. BARRETTE, M. J. LEVINE and P. BRAUN-MUNZINGER, *Phys. Rev. Lett.*, **41**, 1778 (1978).
- [14] S. KUBONO, P. D. BOND and C. E. THORN, *Phys. Lett.*, **81B**, 140 (1979).
- [15] P. BRAUN-MUNZINGER, G. M. BERKOWITZ, M. GAI, C. M. JACHINSKI, T. R. RENNER, C. D. UHLHORN, J. BARRETTE and M. J. LEVINE, *Phys. Rev.*, **C24**, 1010 (1981).
- [16] D. DEHNHARD, V. SHKOLNIK and M. A. FRANEY, *Phys. Rev. Lett.*, **40**, 1549 (1978).

- [17] S. KUBONO, P. D. BOND, D. HORN and C. E. THORN, *Phys. Lett.*, **84B**, 408 (1978).
- [18] U. C. VOOS, W. VON OERTZEN and R. BOCH, *Nucl. Phys.*, **A135**, 571 (1969).
- [19] S. Y. LEE, *Nucl. Phys.*, **A311**, 311 (1978).
- [20] M. PAUL, S. J. SANDERS, J. CSEH, P. F. GESSMAN, W. HENNING, D. G. KOVAR, C. OLMER and J. P. SCHIFFER, *Phys. Rev. Lett.*, **40**, 1310 (1978).
- [21] S. M. LEE, J. C. ADLOFF, P. CHEVALIER, D. DISDIER, V. RAUCH and F. SCHEIBLING, *Phys. Rev. Lett.*, **32**, 429 (1979).
- [22] R. LICHTENTHALER, A. LEPINE-SZILY, A. C. C. VILLARI, W. MITTIG, V. J. G. PORTO and C. V. ACQUADRO, *Phys. Rev.*, **C26**, 2487 (1982).
- [23] U. C. SCHLOTTHAUER-VOOS, R. BOCK, H. G. BOHLEN, H. H. GUTBROD and W. VON OERTZEN, *Nucl. Phys.*, **A186**, 225 (1972).
- [24] G. VOURVOPOULOS, preprint (1984).